Effect of Additives on Dissolution and Swelling of Soybean Lecithin Microcapsules Prepared Using the Wurster Process

Kaori JONO,*[,a] Hideki ICHIKAWA,[a] Yoshinobu FUKUMORI,[a] Ryuichi KANAMORI,[b] Yasuji TSUTSUMI,[b] Katsuko MURATA,[c] Atsuko MORIMOTO,[c] and Kenji NAKAMURA[c]

Faculty of Pharmaceutical Sciences, Kobe Gakuin University,[a] Arise, Ikawadani-cho, Nishi-ku, Kobe 651–21, Japan, Pharmaceutical Department, Itami Municipal Hospital,[b] 1–100 Koya-ike, Itami, Hyogo 664, Japan, and Department of Radiology, Faculty of Medicine, Osaka City University,[c] 1–5–7 Asahi-cho, Abeno-ku, Osaka 545, Japan.
Received June 12, 1997; accepted August 11, 1997

Microcapsules whose membranes contained soybean lecithin (SL), cholesterol (CH), stearic acid (SA) and polyvinylpyrrolidone (PVP) at various compositions were prepared. Then, dissolution and swelling behaviors of the microcapsules in a 0.9% saline solution were studied to be related to the phase diagram of three components containing 42% of PVP in anhydrous state. In the aqueous solution, when an anhydrous microcapsule membrane was composed of SL not saturated with both CH and SA, the microcapsules showed rapid release of carbazochrome sodium sulfonate (CCSS, a model drug), poor particle-swelling and spouting of droplets containing CCSS. Long-delayed release of CCSS and drastic particle-swelling with no spouting of droplets were observed when the anhydrous membrane was composed of SL saturated with both CH and SA and the composition was not close to the two-component line, CH–SA, or to the saturation line. The spouting of droplets would be attributable to the CH and/or SA-poor SL phase and to the SL phase which dissolved CH and SA, but contained either CH or SA only in a small amount, and the delayed release would be due to the CH and SA-rich SL phase dissolving a great amount of CH and SA formed by hydration. The degree of release suppression and particle-swelling depended on the SL content. At 20-45% of SL content, the prolonged-release, great particle-swelling and no spouting of droplets at the early stage were observed only when the CH and SA-rich SL phase formed by hydration contained a high content of CH and SA.

Key words microcapsule; lecithin; controlled release; bioerosion; coating; fluidized bed

Phospholipids have been widely used in pharmaceutical dosage forms such as emulsions,[1] liposomes,[2] solid dispersions[3] and suppositories.[4] These dosage forms utilize the hydration and amphiphilic properties of phospholipids. Soybean lecithin (SL) microcapsules whose membrane was composed of SL, cholesterol (CH), stearic acid (SA) and polyvinylpyrrolidon (PVP) were studied previously by the present authors.[5] The microcapsules were composed of a lactose core (75—106 μm), a drug-layer of carbazochrome sodium sulfonate (CCSS, a model drug) and SL–CH–SA–PVP mixture and a coat of the mixture and were prepared using the Wurster process.[6] The microcapsules exhibited short-term delayed and subsequently prolonged release when the membrane contained all four components, for example, at the weight ratio of SL, CH and SA of 5 : 5 : 2 with 42% of PVP based on the total weight of SL, CH and SA. The dissolution and swelling properties of the microcapsules in a 0.9% saline solution were sensitive to composition of the membrane.

Phase separation in dry SL–CH–SA–PVP membrane mixtures with various compositions was studied on differential scanning calorimetry (DSC), X-ray diffractometry (XRD) and polarizing microscopy.[7] An estimated phase diagram of the SL–CH–SA system containing 42% PVP indicated six regions with the following phase(s): 1) SL liquid crystalline phase (SL(LCP)); 2) SL(LCP) and crystalline CH phase (CH(c)); 3) SL(LCP), CH(c) and crystalline SA phase (SA(c')), which had a pattern with some peaks shifted to shorter spacings compared with the parent SA on XRD; 4) CH(c), SA(c') and crystalline SA phase (SA(c)), which had the same pattern as the parent SA on XRD; 5) SA(c) and SA(c'); 6) SL(LCP) and SA(c'). It was not clear whether SL(LCP) was present in the fourth and fifth zones or not.

In the present study, microcapsules with widely varied membrane composition were prepared to elucidate the effects of SL, CH, SA and PVP on their dissolution and swelling properties. The relation between these microcapsule properties and the phase diagram of anhydrous membrane mixtures is discussed.

Experimental

Materials Lactose (DMV 200M) was sieved into 75—106 μm and used as a core material. SL (reagent grade, about 30% phosphatidylcholine, a minimum of 95% phospholipids) was purchased from Nacalai Tesque Inc., Kyoto, Japan. The phospholipids contained in SL were previously described in detail.[7] CH (guaranteed reagent (GP) grade), SA (GP grade), PVP (K-30, MW = 40000, extra pure reagent grade), methylene chloride and ethanol were used as purchased from Nacalai Tesque, Inc. CCSS, a water-soluble model drug, was supplied by Kanebo, Ltd., Osaka, Japan. Glass beads (200 μm, GB-02, Top Co., Ltd., Kyoto, Japan) were used as a diluent in dissolution tests after washing with ethanol and distilled water.

Coating A Grow Max (140) spouted bed coater with a draft tube (Fuji Paudal Co., Ltd., Osaka, Japan) was used. A spray nozzle of 0.8 mm diameter and a bag-filter with an opening of about 5 μm were employed throughout all experiments.

Preparation of Microcapsules Details of cores, compositions of spray solutions and coating conditions are listed in Table 1. Microcapsules were prepared as previously reported (Table 1).[5] When the materials were difficult to dissolve in methylene chloride–ethanol (1 : 1), methylene chloride was added until a solution was obtained. The composition is denoted below by the weight ratio of SL, CH and SA, and the percent of PVP based on the total weight of SL, CH and SA in parenthesis, like 5 : 5 : 2 (42).

Particle Size Distribution A sieve analysis was performed as previously reported using a row-tap shaker (Iida Seisakusho Co., Ltd., Osaka, Japan).[5]

* To whom correspondence should be addressed.

Dissolution and Drug Content Dissolution tests were performed at 37 °C in a 0.9% saline solution by a column method using HPLC (Shimadzu LC-3A, Kyoto, Japan) and drug content in microcapsules was determined as previously reported.[5,6j] The largest fraction of single-core microcapsules, 149—177 or 177—210 μm, was used. When microcapsules were eroded and some water-insoluble fragments were generated, an increase in absorbance due to turbidity was observed in the dissolution tests with the corresponding placebos. Otherwise, the placebos exhibited no significant level of absorbance.

Polarizing Microscopy An Olympus POM polarizing microscope was used with a heating stage and a temperature controller (LK-600PM, Linkam, Seurrey, UK). Microscopic observations were made of microcapsules (149—177 or 177—210 μm) immersed in a 0.9% saline solution at 37 °C. Microphotographs were taken with a camera (OLYMPUS C-35) attached to the microscope at appropriate time intervals.

Swelling of Microcapsules Using the microphotographs, taken on polarizing microscopy, two diameters (a, b) which did not contain surrounding droplets were measured for a microcapsule. The swelling ratio (SR) was defined by the following equation: $SR=((a_t/a_i)+(b_t/b_i))/2$, where a_t, b_t are the diameters of a microcapsule at the time t and a_i, b_i are the corresponding initial diameters taken at 2 min after immersion, as it took 1 to 2 min to prepare the immersed sample of microcapsules for observation.

Differential Scanning Calorimetry (DSC) Dry samples were prepared as previously reported.[5,7] For hydrated samples, 80 mg of the dry sample was weighed in a glass tube, 400 μl of a 0.9% saline solution was added and incubation followed for 60 min at 37 °C without shaking. After centrifugation at 3000 rpm for 20 min, the supernatant was removed and the paste-like residue was used for the DSC analysis.

A Shimadzu DSC-50 differential scanning calorimeter was used. The onset temperatures of the heating thermograms were considered the temperatures of the peaks as previously reported, unless otherwise mentioned. The hydrated sample of 6—13 mg, except SA, 4 mg, was loaded into an aluminum sample pan, sealed and heated at a rate of 5 °C/min in the temperature range of 20 to 90 °C under a nitrogen flow of 30 ml/min.

Results

Preparation of Microcapsules Forty-three kinds of microcapsules were prepared with various compositions of SL, CH, SA and PVP. The compositions and coating performance in typical cases are listed in Table 1. In spite of variation in physicochemical properties of the membranes, all kinds of microcapsules were prepared with a minor change of operating conditions in the Wurster process. When a weight fraction of CH and/or SA in a membrane was high, liquid flow rate had to be high to avoid spray-drying and adhesion of particles to the wall surface of the coating chamber due to static electricity. The spray solution of 0:0:1 (42) had to be diluted from 750 to 1125 ml, because SA was soon precipitated from the solution in the spray tube. The yield was 87—97% and the mass median diameter was 164—187 μm (Table 1). The lowest yield at 5:5:2 (10) would result from an insufficient amount of binder, PVP. Although drug content of the obtained microcapsules was 1.3—3.8%, it was set at a low level sufficient to monitor drug release properties as previously mentioned.[5]

Effect of SL on Dissolution Dissolution profiles are shown in Fig. 1A, when SL content (X) is changed at X:5:5 (42). At $X=0$ (0:5:5 (42)), CCSS was rapidly released. Addition of a small amount of SL to the membrane significantly suppressed the rapid release ($X=1$,

Table 1. Formulation of Membrane Materials[a] and Coating Performance[b]

No.	Composition[c]	SL (g)	CH (g)	SA (g)	PVP (g)	Yield (%)	Mass median diameter (μm)	Drug content (%)
1	5:5:2 (42)	31.2	31.2	12.6	31.2	97	179	2.4
2	0:5:5 (42)	0	37.5	37.5	31.2	92	177	2.9
3	1:5:5 (42)	6.8	34.1	34.1	31.2	93	176	2.5
4	2:5:5 (42)	12.5	31.3	31.3	31.2	92	175	2.4
5	5:5:5 (42)	25.0	25.0	25.5	31.2	91	169	2.1
6	45:5:5 (42)	61.4	6.8	6.8	31.2	94	179	2.0
7	5:0:2 (42)	53.6	0	21.4	31.2	94	170	2.6
8	5:1:2 (42)	46.9	9.4	18.8	31.2	96	189	2.4
9	5:2:2 (42)	41.7	16.7	16.7	31.2	96	183	2.9
10	5:3:2 (42)	37.5	22.5	15.0	31.2	96	186	2.9
11	5:7:2 (42)	26.8	37.5	10.7	31.2	96	184	2.9
12	5:16:2 (42)	16.3	52.2	6.5	31.2	95	179	2.4
13	5:5:0 (42)	37.5	37.5	0	31.2	95	181	2.2
14	5:5:0.25 (42)	36.6	36.6	1.8	31.2	97	181	2.5
15	5:5:0.5 (42)	35.7	35.7	3.6	31.2	95	178	2.4
16	5:5:0.75 (42)	34.9	34.9	5.2	31.2	96	185	2.8
17	5:5:1 (42)	34.1	34.1	6.8	31.2	94	164	2.7
18	5:5:3 (42)	28.9	28.9	17.3	31.2	93	176	2.7
19	5:5:15 (42)	15.0	15.0	45.0	31.2	89	178	2.1
20	5:5:18.5 (42)	13.2	13.2	48.7	31.2	92	176	2.1
21	5:5:25 (42)	10.7	10.7	53.6	31.2	90	176	2.2
22	5:5:40 (42)	7.5	7.5	60.0	31.2	91	187	2.1
23	5:5:2 (10)	31.2	31.2	12.6	7.5	87	172	3.8
24	5:5:2 (20)	31.2	31.2	12.6	15.0	94	177	3.5
25	5:5:2 (30)	31.2	31.2	12.6	22.5	91	168	3.1
26	5:5:2 (50)	31.2	31.2	12.6	37.5	93	176	1.7
27	5:5:2 (60)	31.2	31.2	12.6	45.0	92	177	1.3

a) Core, 75—106 μm lactose of 25 g. Spray solution, prepared by dissolving the membrane materials in 750 ml of 1:1 ethanol–dichloromethane. Drug, CCSS of 5 g, layered on the cores with 250 ml of the spray solution. The spray solution of 500 ml was overcoated on the drug-layered particles. *b*) Operating conditions: inlet air temperature, 30 °C; outlet air temperature, 21—27 °C; inlet air flow rate, 0.15—0.35 m^3/min; spray air pressure, 2.0—2.8 atm; liquid flow rate, 2.6—6.1 ml/min; nozzle diameter, 0.8 mm. *c*) Total weight of SL, CH and SA is 75 g. The composition is designated by weight ratio of these three compounds and, in parenthesis, by weight percent of PVP based on the total weight of SL, CH and SA.

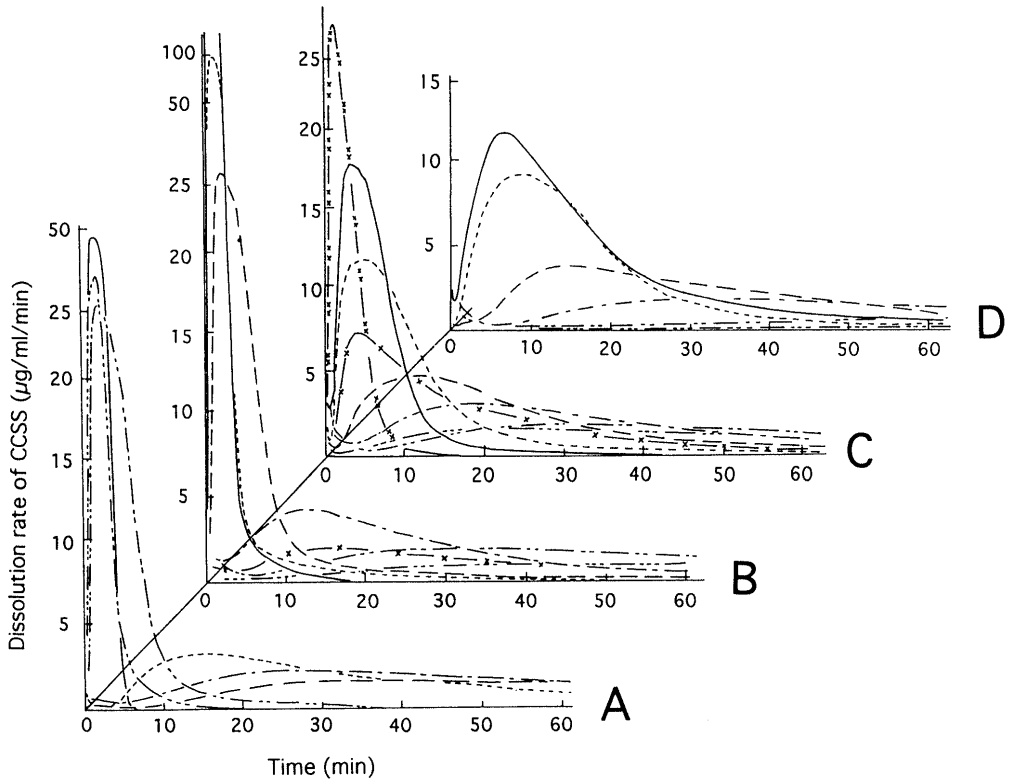

Fig. 1. Effect of SL, CH, SA or PVP on Release of CCSS from Microcapsules in a 0.9% Saline Solution at 37 °C

A) The weight ratio of SL, X, was changed at $X:5:5$ (42): ——, $X=0$; ------, $X=1$; – – –, $X=2$; —·—, $X=5$; —··—, $X=12.5$; —···—, $X=45$. B) The weight ratio of CH, Y, was changed at $5:Y:2$ (42): ——, $Y=0$; ------, $Y=1$; – – –, $Y=2$; —·—, $Y=3$; —··—, $Y=5$; —···—, $Y=7$; —×—, $Y=16$. C) The weight ratio of SA, Z, was changed at $5:5:Z$ (42): ——, $Z=0$; ------, $Z=0.25$; – – –, $Z=0.75$; —·—, $Z=1$; —··—, $Z=2$; —···—, $Z=18.5$; —×—, $Z=25$; —× ×—, $Z=40$. D) The weight percent of PVP, P, was changed at $5:5:2$ (P): ——, $P=10$; ------, $P=20$; – – –, $P=30$; —·—, $P=42$; —··—, $P=50$; —···—, $P=60$. Size fraction of microcapsules used in dissolution tests: $P=10$, 20 and 30, 149—177 μm; others, 177—210 μm.

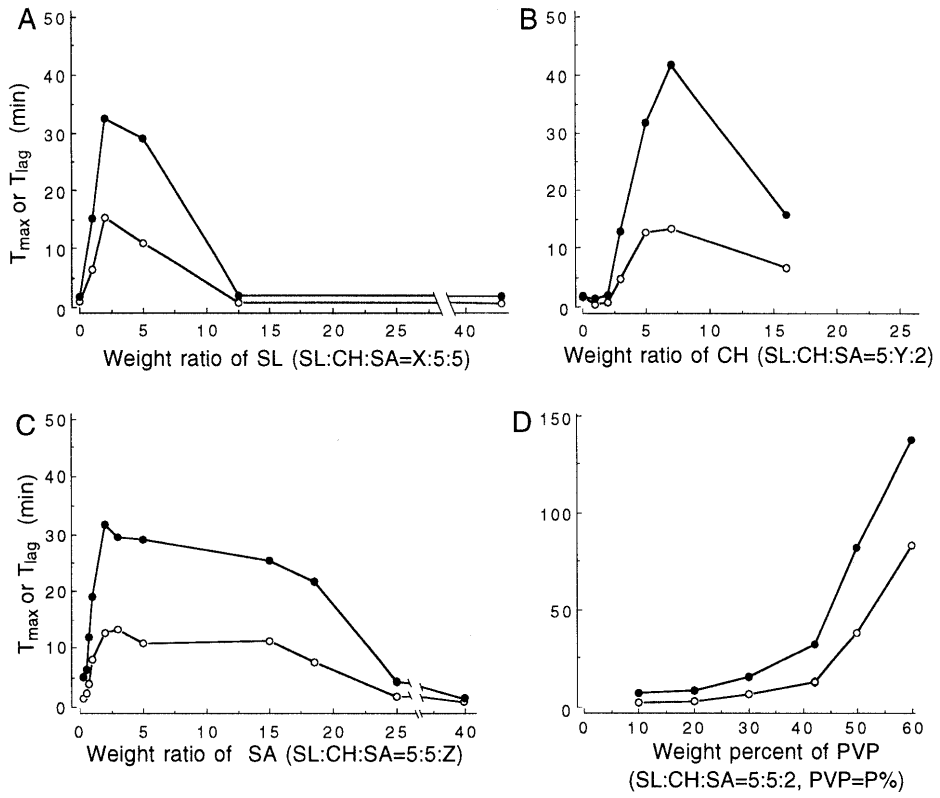

Fig. 2. Effect of SL, CH, SA or PVP on T_{max} and T_{lag} of Microcapsules in a 0.9% Saline Solution at 37 °C

●, T_{max}; ○, T_{lag}. A) The weight ratio of SL, X, was changed at $X:5:5$ (42). B) The weight ratio of CH, Y, was changed at $5:Y:2$ (42). C) The weight ratio of SA, Z, was changed at $5:5:Z$ (42). D) The weight percent of PVP, P, was changed at $5:5:2$ (P). Size fraction of microcapsules used in dissolution tests: $P=10$, 20 and 30, 149—177 μm; others, 177—210 μm.

1:5:5 (42)). The release was most suppressed at $X=2$ (2:5:5 (42)). At more than $X=2$, however, the release rate began to increase, and rapid release was again seen as SL reached $X=12.5$ (5:2:2 (42)). When SL increased further to $X=45$ (45:5:5 (42)), the release profile was similar to that at $X=0$.

Dissolution parameters, T_{max} and T_{lag},[5] are plotted against X in Fig. 2A; T_{max} was the time at the maximum dissolution rate and T_{lag} was the time when the dissolution rate reached half of the maximum rate. These increased to 32.5 and 15.3 min, respectively, at $X=2$, above which they gradually decreased.

Effect of CH on Dissolution The release profiles are shown in Fig. 1B, when CH content (Y) is changed at 5:Y:2 (42). T_{max} and T_{lag} are plotted against Y in Fig. 2B. The membrane without CH ($Y=0$, 5:0:2 (42)) had no ability to control release of CCSS (Fig. 1B). As CH increased, the release was further suppressed, and the strongest suppression was found at $Y=7$ (5:7:2 (42)). T_{max} and T_{lag} at $Y=7$ were 41.5 and 13.2 min, respectively (Fig. 2B). Above $Y=7$, the release rate tended to increase with CH (Fig. 1B).

Effect of SA on Dissolution The release profiles are shown in Fig. 1C, when SA content (Z) is changed at 5:5:Z (42). T_{max} and T_{lag} are plotted against Z in Fig. 2C. The membrane of $Z=0$ (5:5:0 (42)) had slight ability to suppress release of CCSS, different from those at $X=0$ (Fig. 1A) and $Y=0$ (Fig. 1B). The release was most suppressed at $Z=2$ and 3 (5:5:2 (42) and 5:5:3 (42), Fig. 1C). The maxima of T_{max} and T_{lag} were 31.7 min at $Z=2$ and 13.3 min at $Z=3$, respectively (Fig. 2C). When SA was more than $Z=2$, however, the release rate was kept low up to $Z=18.5$ (5:5:18.5 (42)). At $Z=25$ (5:5:25 (42)) or more ($Z=40$, 5:5:40 (42)), the release rate became very high.

Effect of PVP on Dissolution Release profiles are shown in Fig. 1D, when the weight percent of PVP (P) based on the total weight of SL, CH and SA is changed at 5:5:2 (P). T_{max} and T_{lag} plotted against P in Fig. 2D increased monotonously, and remarkably increased when PVP was above $P=42$ (5:5:2 (42)).

Effect of SL on Swelling Microcapsules immersed in a 0.9% saline solution were observed using a polarizing microscope at 37 °C (Figs. 3 and 4). SL content (X) was changed at X:5:5 (42) (Figs. 3a—f and 4A). At $X=0$ (0:5:5 (42)), microcapsules were little swollen (Fig. 4A) and retained almost the same shape for 60 min (Figs. 3a and 3b) with a burst of CCSS release (Fig. 1A): the

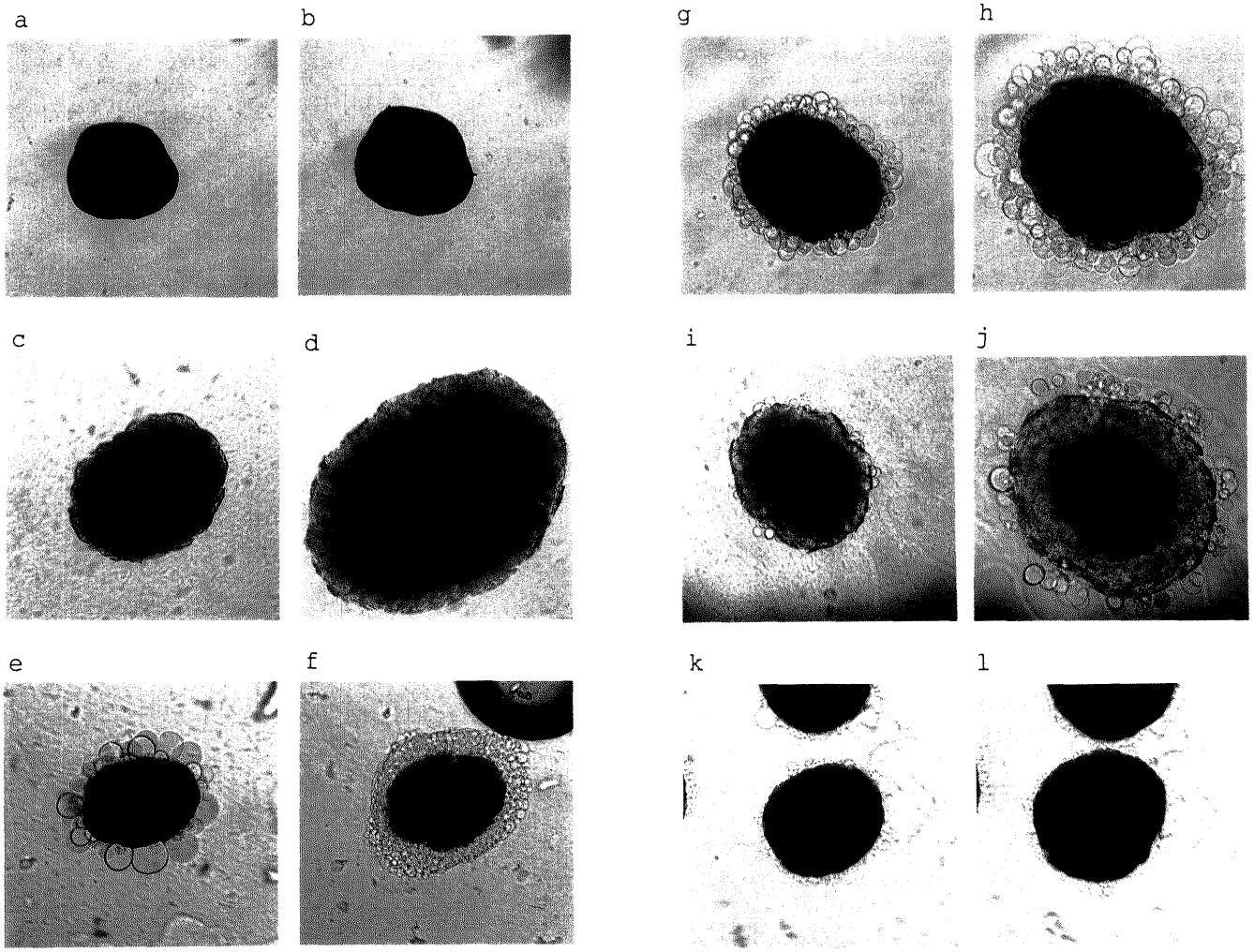

Fig. 3. Microphotographs of Microcapsules Immersed in a 0.9% Saline Solution at 37 °C

Microcapsules [time (min) after initial immersion]: a, 0:5:5 (42) [3]; b, 0:5:5 (42) [60]; c, 5:5:5 (42) [3]; d, 5:5:5 (42) [60]; e, 5:2:2 (42) [3]; f, 5:2:2 (42) [60]; g, 5:5:0.25 (42) [3]; h, 5:5:0.25 (42) [60]; i, 5:5:0.75 (42) [3]; j, 5:5:0.75 (42) [60]; k, 5:5:25 (42) [3]; l, 5:5:25 (42) [60].

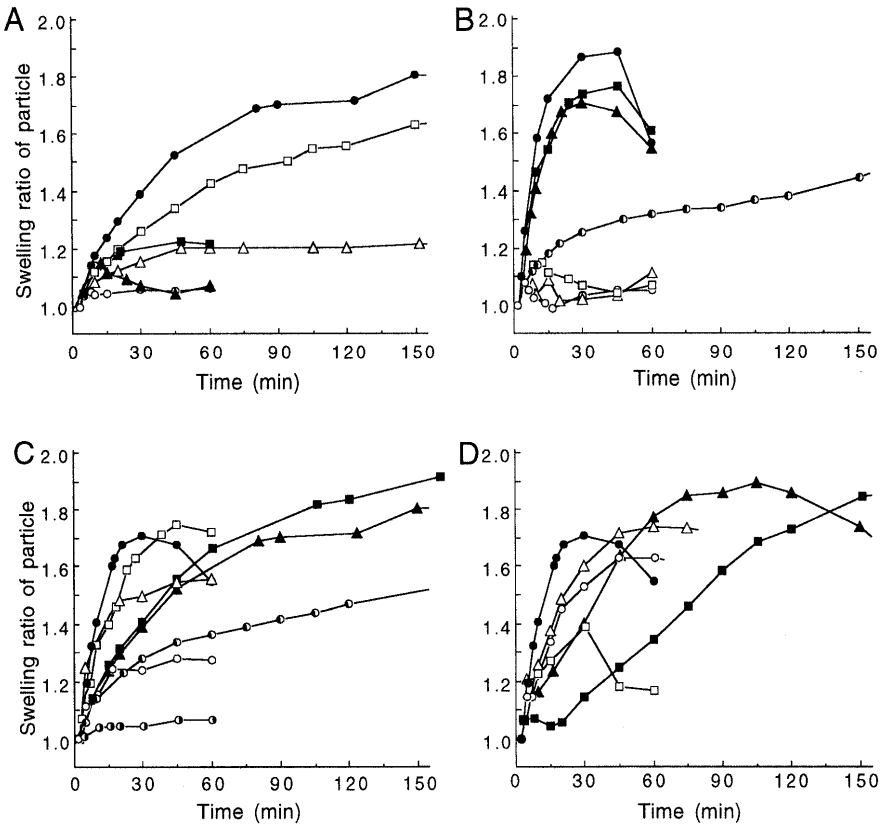

Fig. 4. Effect of SL, CH, SA or PVP on SR of Microcapsules in a 0.9% Saline Solution at 37 °C

A) The weight ratio of SL, X, was changed at X: 5 : 5 (42): ○, $X=0$; △, $X=1$; □, $X=2$; ●, $X=5$; ▲, $X=12.5$; ■, $X=45$. B) The weight ratio of CH, Y, was changed at 5 : Y : 2 (42): ○, $Y=0$; △, $Y=1$; □, $Y=2$; ●, $Y=3$: ▲, $Y=5$; ■, $Y=7$; ◐, $Y=16$. C) The weight ratio of SA, Z, was changed at 5 : 5 : Z (42): ○, $Z=0$; △, $Z=0.25$; □, $Z=1$; ●, $Z=2$; ▲, $Z=5$; ■, $Z=15$; ◐, $Z=18.5$; ◑, $Z=40$. D) The weight percent of PVP, P, was changed at 5 : 5 : 2 (P): ○, $P=10$; △, $P=20$; □, $P=30$; ●, $P=42$; ▲, $P=50$; ■, $P=60$. Size fraction of microcapsules used in dissolution tests: $P=10$, 20 and 30, 149—177 μm; others, 177—210 μm.

maximum SR (MSR) was 1.1 at 30 min (Fig. 4A). At $X=1$ (1 : 5 : 5 (42)), microcapsules increased in size for 45 min by swelling and thereafter their sizes remained almost constant (MSR = 1.3 at 330 min, Fig. 4A), showing delayed release of CCSS with a clear lag time (Fig. 1A). At $X=2$ (2 : 5 : 5 (42)), microcapsules were greatly swollen, but this occurred slowly (Fig. 4A) with more delay of the release (Fig. 1A). SR reached 2.1 at 400 min, still with swelling (Fig. 4A). As SL increased above $X=2$, the swelling became more rapid and was less than at $X=2$: MSR = 1.8 at 150 min with microcapsules at $X=5$ (Figs. 3c, 3d and 4A). Droplet-like materials were observed to spout out from microcapsules immediately after immersion as SL reached $X=12.5$ (5 : 2 : 2 (42), Fig. 3e). The droplets were yellow, clearly coming from dissolved CCSS, and greatly swollen; they moved away from the microcapsules until 10 min of immersion and thereafter many small and colorless droplets remained around the microcapsules (Fig. 3f). The microcapsules at $X=12.5$ showed more rapid release of CCSS (Fig. 1A) and less swelling than those at $X=5$, and small MSR of 1.2 was found at 10 min (Fig. 4A). At $X=45$ (45 : 5 : 5 (42)), MSR was 1.2 at 45 min. Spouting of the yellow droplets was also observed immediately after immersion, they gradually decreased in number and only a few droplets were observed at 30 min. No small, colorless droplets remained at $X=45$. In all microcapsules whose SL content (X) was changed at X : 5 : 5 (42) except for $X=0$ and 1, they gradually eroded after SR reached MSR. These results indicated that although the swelling was induced by SL as expected, an excess amount of SL as great as $X=12.5$ and 45 induced a spouting of the contents rather than swelling.

Effect of CH on Swelling CH content (Y) was changed at 5 : Y : 2 (42) (Figs. 3e, 3f and 4B). At $Y=0$ (5 : 0 : 2 (42)), a few small droplets were spouted out immediately and moved away from microcapsules a few minutes after immersion, as shown in a previous paper.[5] However, it was not clear whether the droplets were yellow or not, since the aqueous medium became yellow immediately after immersion, well corresponding to the immediate release on the dissolution tests (Fig. 1B). Thereafter, many small and colorless droplets remained around the microcapsules as seen in Fig. 3f with only a slight change of SR: MSR at $Y=0$ was 1.1 at 45 min (Fig. 4B). Many yellow droplets were also observed to spout out from microcapsules at $Y=1$ (5 : 1 : 2 (42)) and $Y=2$ (5 : 2 : 2 (42), which corresponded to $X=12.5$, Figs. 3e and 3f). The appearance of the small, colorless droplets around the microcapsules and the value of MSR were similar to those at $Y=0$ (Fig. 4B). At $Y=3$ (5 : 3 : 2 (42)), $Y=5$ (5 : 5 : 2 (42)) and $Y=7$ (5 : 7 : 2 (42)), microcapsules were greatly swollen (Fig. 4B), with slower release of CCSS (Fig. 1B). After reaching MSR, SR remarkably decreased (Fig. 4B). Only a small number of droplets, which were not clearly yellow and almost colorless, initially spouted out from the microcapsules, and thereafter the spouting occurred most frequently around 45 min at $Y=3$. The initial spouting at $Y=5$ and 7 was more delayed than that at $Y=3$, and most

frequently observed around 40 min. MSRs at $Y=3$, 5 and 7 were 1.9 at 45 min, 1.7 at 30 min and 1.8 at 45 min, respectively (Fig. 4B). At $Y=16$ (5 : 16 : 2 (42)), the swelling was much slower than that at $Y=3$, 5 and 7, but the release of CCSS was less delayed (Fig. 1B). SR increased to 2.0 at 420 min still with swelling. The spouting of droplets was no longer observed at $Y=16$. These results indicated that when the membrane composition was altered at 5 : Y : 2 (42), increase in hydrophobic CH up to $Y=7$ delayed spouting from the microcapsules along with enhanced swelling, but too much CH led to less delay of release in spite of the still enhanced swelling.

Effect of SA on Swelling SA content (Z) was changed at 5 : 5 : Z (42) (Figs. 3c, 3d, 3g—l and 4C). A large number of yellow droplets were observed to spout out from microcapsules immediately after immersion at $Z=0$ (5 : 5 : 0 (42)), as shown previously,[5] with rapid release of CCSS (Fig. 1C). This was followed by spouting of a lesser number of the droplets, which became almost colorless, around 15 min. The microcapsules at $Z=0$ were only slightly swollen and MSR was 1.3 at 45 min (Fig. 4C). At $Z=0.25$ (5 : 5 : 0.25 (42)), spouting of the yellow droplets was more frequently observed (Fig. 3g), and spouting of a large number continued until 60 min of immersion (Fig. 3h). With such a small amount of SA as $Z=0.25$, swelling of the microcapsules was enhanced, and MSR reached 1.6 at 45 min (Fig. 4C). At $Z=0.5$ and 0.75 (5 : 5 : 0.5 (42) and 5 : 5 : 0.75 (42)), the spouting was significantly suppressed, whereas it continued even at 60 min (Fig. 3j). Especially, the spouting at the early stage after immersion began to be delayed at $Z=0.5$ and the spouting had a short lag time of about 5 to 10 min at $Z=0.75$ (Fig. 3i), accompanied by an increase in T_{lag} (Fig. 2C). Spouting of the yellow droplets was infrequent at $Z=1$ (5 : 5 : 1 (42)), as shown previously,[5] with a great swelling (Fig. 4C) and slower release of CCSS (Fig. 1C). Instead of the yellow droplets, many droplets which seemed to be almost colorless were observed at $Z=1$ around 20 min after immersion. MSR at $Z=1$ was 1.8 at 45 min (Fig. 4C). At $Z=2$ (5 : 5 : 2 (42), which corresponded to $Y=5$), many almost colorless droplets began to spout out from microcapsules around 20 min and were most frequently observed around 40 min after immersion. At $Z=2$, MSR was 1.7 at 30 min. When SA increased to $Z=5$ (5 : 5 : 5 (42), which corresponded to $X=5$), no more spouting of either type of droplets was seen (Figs. 3c and 3d). The microcapsules at $Z=5$ were more greatly and slowly swollen: MSR was 1.8 at 150 min (Fig. 4C). Microcapsules at $Z=15$ (5 : 5 : 15 (42)) were much more swollen at a slower rate: MSR reached 2.1 at 300 min, which was largest in the 5 : 5 : Z (42) microcapsules. Nor was any spouting of droplets observed at $Z=15$. When SA increased to $Z=18.5$ (5 : 5 : 18.5 (42)), a very slight number of small and almost colorless droplets were again observed to spout out from microcapsules and the spouting was slightly increased around 20 min. MSR began to lower and the swelling to slow down as SA increased beyond $Z=15$, with an enhanced release of CCSS (Fig. 1C). MSR at $Z=18.5$ was 1.9 at 500 min (Fig. 4C). The droplets spouted out from microcapsules at $Z=25$ (5 : 5 : 25 (42), Figs. 3k and 3l) were almost colorless, but gradually became yellow. MSR at $Z=25$ reduced to 1.2 at 380 min (data not shown). At $Z=40$, no droplet was observed and microcapsules were little swollen (MSR = 1.1 at 45 min, Fig. 4C), but the release of CCSS became very rapid (Fig. 1C). These results indicated that below about $Z=18.5$ SA essentially suppressed droplet spouting and enhanced swelling, leading to delayed and prolonged release, but too much SA (above $Z=18.5$) induced the spouting again, except at $Z=40$.

Effect of PVP on Swelling PVP content (P) was changed at 5 : 5 : 2 (P). At $P=10$ (5 : 5 : 2 (10)), very small droplets were observed to spout from microcapsules immediately after immersion with rapid release of CCSS (Fig. 1D). It was not clear at first whether they were yellow or not, but they gradually became visibly yellow. Thereafter, the droplets gradually increased in number until around 45 min. The microcapsules at $P=10$ were greatly swollen and MSR was 1.6 at 45 min (Fig. 4D). Appearance and the drug release (Fig. 1D) of microcapsules at $P=20$ (5 : 5 : 2 (20)) were similar to those at $P=10$, but the microcapsules exhibited more swelling: MSR was 1.7 at 60 min (Fig. 4D). At $P=30$ (5 : 5 : 2 (30)), the yellow droplets were no longer observed, but spouting of many colorless droplets began after a delay of around 10 min. In this case, the initial release of CCSS was significantly suppressed (Fig. 1D). Spouting of the colorless droplets was enhanced around 30 min and thereafter continued until 60 min. The microcapsules at P = 30 were greatly swollen, but began to reduce in size around 30 min (Fig. 4D), with frequent spouting of colorless droplets. As a result, MSR at $P=30$ was small, 1.4 at 30 min. At $P=42$ (5 : 5 : 2 (42), which corresponded to $Y=5$ and $Z=2$), microcapsules were extremely swollen as observed at $P=$ 10 and 20, but the spouting of yellow droplets was not observed at the early stage, as shown previously.[5] Instead, colorless droplets were observed around 20 min after immersion and more frequently around 40 min. During these swelling behaviors, the release of CCSS was greatly prolonged (Fig. 1D). At $P=50$ and 60 (5 : 5 : 2 (50) and 5 : 5 : 2 (60)), microcapsules were more slowly and greatly swollen (Fig. 4D), and no spouting of either type of droplets was observed. MSR was 1.9 at 105 min with $P=50$. SR was 2.0 at 255 min with $P=60$, and still increasing. Above $P=42$, the release of CCSS was strongly suppressed (Fig. 1D). These results showed that 30% of PVP suppressed spouting of CCSS-containing droplets, and at higher content suppressed erosion, leading to the large swelling and the delayed and prolonged release.

Relation of Dissolution and Swelling Behaviors with the Phase Diagram T_{lag} (Fig. 2) and MSR (Fig. 4) are plotted on the phase diagram of anhydrous SL–CH–SA systems containing 42% PVP in Fig. 5.[7] Detail of the six regions in the diagram was discussed in the previous paper.[7] Point F shows the composition of 5 : 5 : 2 (42). The large and small plots in the diagram show measured and interpolated points, respectively. The closed plots show the compositions where spouting of droplets was observed at the early stage.

Dissolution behaviors are illustrated on the phase diagram using only T_{lag} (Fig. 5A), because T_{max} and T_{lag} changed in almost the same way as seen in Fig. 2, and it was difficult to correctly determine T_{max} when a dissolution

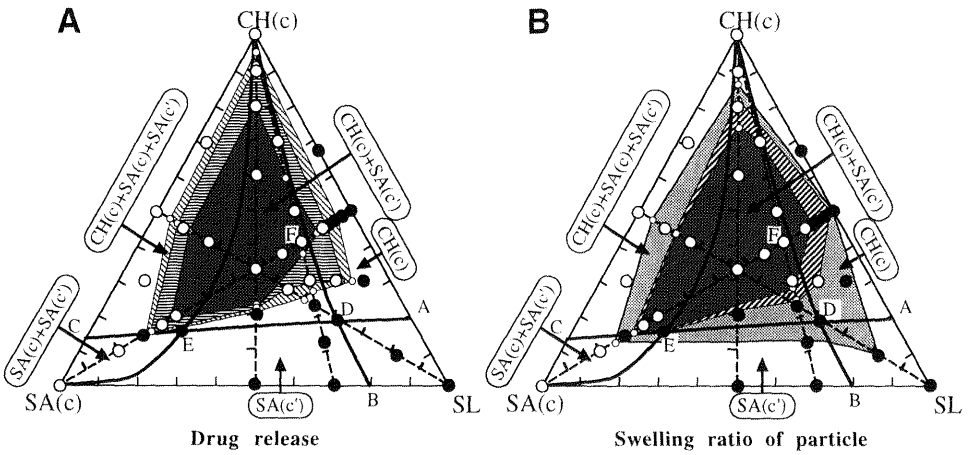

Fig. 5. T_{lag} (A) and MSR (B) Plotted on Phase Diagram of SL–CH–SA System with 42% PVP in Anhydrous State

The large plots, measured; the small, interpolated. Closed symbols, the microcapsules from which spouting of droplets was observed at the early stage in a 0.9% saline solution by microscopy; open, other microcapsules. Separation of crystalline phase(s) detected by DSC or XRD: zone SL-A-D-B, none; zone CH(c)-A-D, CH(c); zone SA(c)-B-D-E, SA(c'); zone SA(c)-E-C, SA(c) and SA(c'); zone CH(c)-C-E, CH(c), SA(c) and SA(c'); zone CH(c)-D-E, CH(c) and SA(c'). A) open region, $T_{lag} < 3$ min; coarsely striped region, 3 min $\leqq T_{lag} < 5$ min; finely striped region, 5 min $\leqq T_{lag} < 10$ min; darkest region, 10 min $\leqq T_{lag}$. B) open region, MSR < 1.2; slightly shadowed region, $1.2 \leqq$ MSR < 1.5; striped region, $1.5 \leqq$ MSR < 1.7; darkest region, MSR $\geqq 1.7$.

rate profile was flat.[5] The dissolution behaviors were as follows: in the open region ($T_{lag} < 3$ min), drug release almost burst and finished in about 40 min; in the coarsely stripped region ($3 \leqq T_{lag} < 5$), the release did not burst and had a short lag time; in the finely stripped region ($5 \leqq T_{lag} < 10$), prolonged release was seen with a lag time followed by a slightly rapid release; in the darkest region ($10 \leqq T_{lag}$), greatly prolonged release was observed. The longest T_{lag} was 75 min with microcapsules of 1 : 3 : 1 (42), except that 1 : 8 : 1 (42) microcapsules showed almost a first-order release without T_{lag} (data not shown).

MSR was used to illustrate swelling behaviors of microcapsules on the phase diagram (Fig. 5B). In the open region (MSR < 1.2), microcapsules were little swollen and their sizes were little enlarged in the solution, while in the darkest region (MSR $\geqq 1.7$), they were extremely swollen. Spouting of droplets was usually observed on the microcapsules whose membrane had composition in the region of MSR < 1.7. The largest MSRs obtained in this study were 2.2 with microcapsules at 24 : 17 : 59 (42), 2.1 at $Z = 15$ and 2.0 at $X = 2$, $Y = 16$ and $P = 60$, though SR was still increasing at the end of the observation period in the latter three.

Discussion

Structural Aspects The amount of SL, CH or SA dissolved in PVP cast film was determined as less than 3, 3 or 1%, respectively, by observation of film-transparence and polarizing microscopy (data not shown). Therefore, most of the SL, CH and SA would be separated in anhydrous state from PVP in the microcapsule membranes prepared in this study. On the other hand, although the amount of PVP which could be dissolved in SL was not clearly determined by the same observations due to difficulty in detection of isotropic PVP in the non-uniform SL film under the polarizing microscope, it would also be very low, because whenever DSC was carried out with or without PVP for the same SL–CH–SA mixtures, PVP seemed not essentially to affect their thermal behaviors.[7]

PVP accounted for 29.6% (v/v) of SL : CH : SA (42) membranes in anhydrous state assuming that all components had the same density. Based on the percolation theory, this PVP fraction could be very close to the lower percolation threshold, meaning that there was only a small amount of PVP phase whose clusters were spanning through the membrane, even if the spanning clusters existed; the other SL, CH and SA phases would constitute the spanning clusters open to the outside of the membranes instead.[8]

The structures of dry membranes would be reconstructed in more or less degree during hydration as a result of water-permeation, swelling, dissolution, release of components from membrane and formation of water-containing stable phases. It was very difficult to clearly elucidate these complicated dynamic-processes. However, estimation of possible structural and physico-chemical features of the processes and the hydrated states was attempted below. DSC studies on the precipitates from the membrane-mixture suspensions in the aqueous solution after 60 min of immersion were considered to be useful, since they would reflect the nearly final stage of the reconstruction processes in the hydrated membranes (Figs. 6 and 7).

Apexes of Phase Diagram Microcapsules of 1 : 0 : 0 (42), 0 : 1 : 0 (42) and 0 : 0 : 1 (42), whose membranes were composed of only one component containing 42% PVP, were studied first. Microcapsules composed only of SL (1 : 0 : 0 (42)) showed a rapid burst in drug release and spouted large droplets immediately after immersion, as reported.[5] The droplets were initially yellow, which came from CCSS, and thereafter the aqueous solution around the microcapsules soon became yellow. The droplets expanded rapidly and grew into one large droplet which surrounded the microcapsules. The microcapsules gradually eroded, accompanied by further growth of the surrounding droplet. These observations well corresponded to the rapid release from the microcapsules. The strong swelling of SL and the dissolution of PVP seemed to account for these results. Microcapsules of both 0 : 1 : 0 (42) and 0 : 0 : 1 (42), on the other hand, also showed a burst in dissolution tests

(data not shown); however, they did not swell at all and spouted nothing, retaining their shapes after immersion. The dissolution of PVP and the consequent porous-structure containing SA or CH crystals would be responsible for these behaviors. These results indicated that the microcapsules composed of only SL, CH or SA containing 42% PVP had no ability to control the drug release, and that those prepared without SL could not swell in the aqueous solution.

SL-A-D-B Region In this region there existed only SL(LCP), which dissolved both CH and SA completely in anhydrous membrane mixtures (Fig. 5). However, SL(LCP) was not saturated with them. The microcapsules showed rapid release and slight swelling in the solution as seen at $X=45$ (45 : 5 : 5 (42), Figs. 1A, 2A and 4A). Spouting of yellow droplets, which were smaller than those at 1 : 0 : 0 (42), was observed immediately after immersion, leading to a burst of CCSS release.

There are many studies on molar ratios of a lecithin–CH complex, association or incorporation in the range from 4 : 1 to 1 : 2 in hydrous state using various lecithins and analytical methods.[9] Phillips and Finer reported from NMR and calorimetric studies that lecithin–CH bilayers contained two phases and that 1 : 1 stoichiometry of lecithin–CH complex separated out clusters of free lecithin molecules in hydrous state when the bilayer contained less than equimolar amount of CH.[9c] McMullen and McElhaney,[9b] and Mabrey *et al.*[9a] also indicated the existence of CH-poor dipalmitoylphosphatidylcholine (DPPC) or pure DPPC domains and CH-rich DPPC domains in a hydrous mixture of DPPC and CH, when the CH concentration was approximately 1—2 to 20—25 mol% or below 20 mol%. Both groups interpreted an asymmetric DSC endotherm corresponding to a main phase transition of DPPC as coexistence of a sharp and a broad melting component; the former came from CH-poor DPPC or pure DPPC domains and the latter from CH-rich DPPC domains. When the molecular weight of SL used here was assumed to be the same as DPPC, the CH concentration in membrane mixtures was below about 30 mol% against the total of SL and CH in this region. Therefore, there would be a potential in this region for the CH-rich SL and the CH-poor SL domains to have been formed in the hydrous membrane, although SA and PVP were contained in the membrane in the present study.

Mixtures of SL and CH containing 42% PVP in a 0.9% saline solution were studied on DSC (Fig. 6A). Because of SL in liquid crystalline phase (Fig. 6A a),[7] the formation of the CH-poor SL and the CH-rich SL phases in this region could not be confirmed. However, it was clear that crystalline CH was not separated in the hydrous membrane mixture in this region (Fig. 6A b).

Schullery *et al.* analyzed mixtures of DPPC and SA in excess water by differential thermal analysis (DTA) and reported that they formed a sharp melting complex with 66 mol% of SA under this condition.[10] In DTA thermograms, a new peak appeared above 41.5 °C, where an endothermic peak of a main transition of DPPC appeared, simultaneously shifted to higher temperatures, and grew at the expense of the original main transition when mole fractions of SA were increased. The peak became sharper and its thermal behavior was similar to pure SA above 0.66 mol fraction of SA. The phase diagram by Schullery and his colleagues indicated that as SA was increased in the mixture composed of DPPC with liquid-crystal structure and SA, a liquid-crystal solution of SA in DPPC was first formed, and subsequently coexisted with a gel solid solution of DPPC in a 1 : 2 complex of DPPC–SA (C-phase); further, at higher SA content, there existed only C-phase and this finally coexisted with SA crystals above 67 mol% of SA. Mabrey and Sturtevant reported that in a 1 : 2 molar ratio mixture of DPPC and SA, SA could not be packed well into a DPPC lattice because of a difference in the chain length of each acyl group.[11] Zuidam and Crommelin reported that palmitic acid (PA) produced by hydrolysis of DPPC–liposome was retained within a lipid bilayer forming several domains which differed in PA content.[12]

To confirm formation of a SL–SA complex, DSC was carried out in this study with mixtures of SL and SA containing 42% PVP hydrated in a 0.9% saline solution (Fig. 6B). An endothermic peak appeared at 41 °C with SL : SA = 5 : 1 mixture (Fig. 6B b). The peak was shifted to higher temperature as SA was increased (Fig. 6B c—e). At SL : SA = 6 : 4, the peak was detected at 62 °C (Fig. 6B f); above SL : SA = 6 : 4 it became sharper and showed no more shift with SA content (Fig. 6B f—h). The temperature at the top of the peak was almost the same as that at SL : SA = 0 : 10 (Fig. 6B i). Although there was a little difference in the temperature where the peaks appeared, peak behaviors with the SL–SA mixtures were similar to those with DPPC and SA reported by Schullery *et al.*[10] There seemed to be two peaks with the mixture of SL : SA = 13 : 7, 6 : 4, 5 : 5 or 4 : 6 (Fig. 6B e—h): the peak which appeared at 41 °C with SL : SA = 5 : 1 mixture and was shifted to higher temperatures by the incorporation of SA, and the other peak at 67 °C which was the same as that at SL : SA = 0 : 10. It was reasonable to consider that the latter peak at 67 °C came from SA crystals separated from the mixture. This phase is referred to below as "SA phase". The former peak which appeared at 41 °C with SL : SA = 5 : 1 mixture and shifted to higher temperatures, finally to 62 °C, with increase in SA might be due to formation of SL–SA complex(es) (SA-rich SL phase) in hydrous state. When the molecular weight of SL was assumed to be the same as that of DPPC, the SA content would be 63 mol% at SL : SA = 6 : 4 where SA phase clearly appeared first (Fig. 6B f), well corresponding to the 1 : 2 complex formation. It was not clear where the border between the existence of C-phase alone and coexistence of liquid-crystal solution of SA in SL (SA-poor SL phase) and C-phase was, , because of the undetectable transition temperature of gel to liquid crystalline phase of SL. The same behavior was observed when hydrous SL– SA mixtures without PVP were studied on DSC (data not shown). Therefore, appearance of the lower temperature peaks was not caused by PVP.[7] Differences of the peak temperature between the results of Schullery *et al.* and Fig. 6B would be due to the fact that SL used in our studies had a variety of acyl chain lengths, saturation degrees and types of phospholipids. With a hydrous membrane mixture at $X=45$ in this region, a

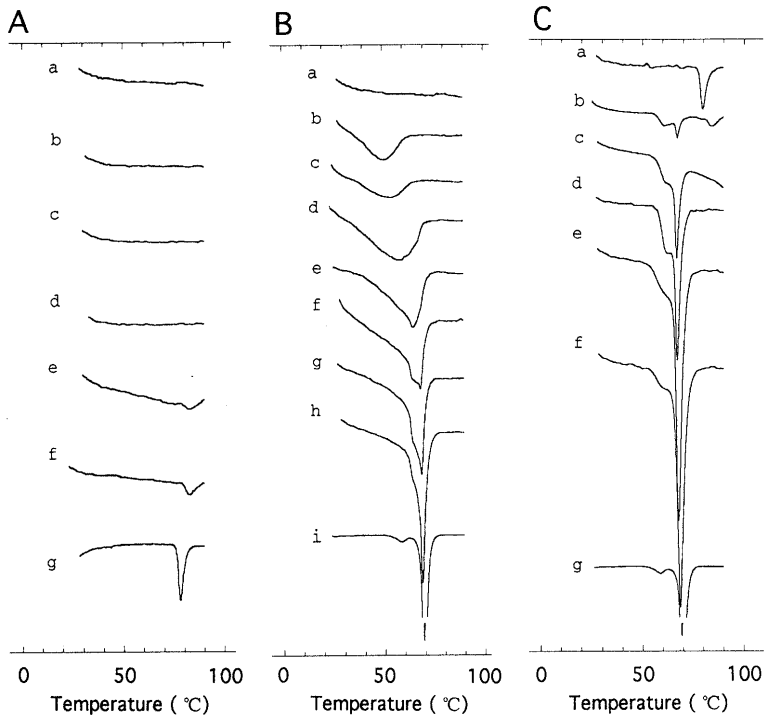

Fig. 6. DSC Thermograms of Hydrated SL–CH (A), SL–SA (B) and CH–SA (C) Mixtures Incorporating 42% PVP

A) The weight ratio of SL and CH (PVP, %): a, 10:0 (42); b, 82:18 (42); c, 5:2 (42); d, 6:4 (42); e, 5:5 (42); f, 1:2 (42); g, 0:10 (42). B) The weight ratio of SL and SA (PVP, %): a, 10:0 (42); b, 5:1 (42); c, 5:1.25 (42); d, 5:2 (42); e, 13:7 (42); f, 6:4 (42); g, 5:5 (42); h, 4:6 (42); i, 0:10 (42). C) The weight ratio of CH and SA (PVP, %): a, 10:0 (42); b, 9:1 (42); c, 3:1 (42); d, 5:5 (42); e, 3:7 (42); f, 1:9 (42); g, 0:10 (42).

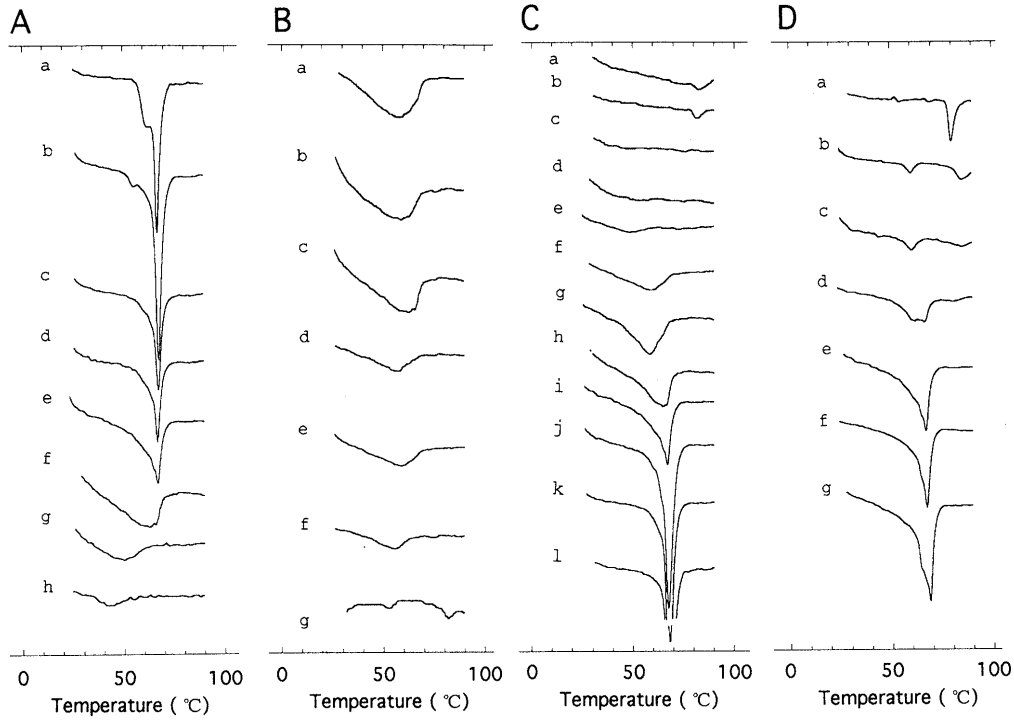

Fig. 7. DSC Thermograms of Hydrated SL–CH–SA Mixtures Incorporating 42% PVP

A) The weight ratio of SL, X, was changed at X:5:5 (42): a, $X=0$; b, $X=1$; c, $X=2$; d, $X=3$; e, $X=5$; f, $X=12.5$; g, $X=25$; h, $X=45$. B) The weight ratio of CH, Y, was changed at 5:Y:2 (42): a, $Y=0$; b, $Y=1$; c, $Y=2$; d, $Y=3$; e, $Y=5$; f, $Y=7$; g, $Y=16$. C) The weight ratio of SA, Z, was changed at 5:5:Z (42): a, $Z=0$; b, $Z=0.25$; c, $Z=0.5$; d, $Z=0.75$; e, $Z=1$; f, $Z=2$; g, $Z=3$; h, $Z=4$; i, $Z=5$; j, $Z=15$; k, $Z=25$; l, $Z=40$. D) The weight ratio of SL, CH and SA (PVP, %): a, 0:1:0 (42); b, 0.5:9:0.5 (42); c, 1:8:1 (42); d, 1:3:1 (42); e, 5:5:5 (42); f, 2:1:2 (42); g, 5:0:5 (42).

broad and small endothermic peak was observed at 45 °C on DSC, suggesting the formation of the SL–SA complex (Fig. 7A h). These results suggested that the hydrated membrane in this SL-A-D-B region would have a potential to form the CH and SA-poor SL, the CH-rich SL, and the SA-rich SL phases. It was not clear whether the latter two would form different phases or one phase rich in both CH and SA. Incorporation of CH and/or SA in SL and formation of these phases in hydrous state might be concerned with the smaller droplets produced in this region.

SA(c)-B-D-E Region The behaviors of the microcapsules prepared at $Y=0$ and 1 (5:0:2 (42) and 5:1:2 (42)) in this region were essentially similar to those in the SL-A-D-B region (Figs. 1B, 2B and 4B). The only difference was in the fact that sizes of the microcapsules at $Y=0$ and 1 were gradually reduced with small, colorless droplets remaining at the final stage (Fig. 4B), while the size remained constant at $X=45$ in the SL-A-D-B region (Fig. 4A). This suggested that the microcapsules at $Y=0$ and 1 would be rapidly eroded, releasing their membrane materials as the small, colorless droplets in the solution. The sizes of the microcapsules at 5:0:5 (42) were slightly increased with spouting of a very small number of droplets at the early stage, although no small, colorless droplets at the final stage were observed (data not shown but plotted in Fig. 5).

In this region, SL(LCP) and separated SA(c′) existed in anhydrous membrane mixtures (Fig. 5). SL(LCP) was saturated with SA, but not with CH. It seemed that when microcapsule membranes contained SL(LCP) which was saturated with only SA in anhydrous state, they also had a poor ability to prolong the release and to swell in the solution, similar to those in the SL-A-D-B region. The effect of increase in CH, which was dissolved in the SL(LCP) in the anhydrous membrane mixture, was not clear in this region.

When microcapsule membranes in the right side of this region (probably the right of SL:SA=6:4) were hydrated, there would also be a potential for formation of the CH and SA-poor SL, the CH-rich SL and the SA-rich SL phases in the membrane. While SA was separated at SL:SA=5:1.25 in anhydrous state on DSC and XRD,[7] it seemed to be first observed at lower SL content, SL:SA=6:4, in hydrous state on DSC (Fig. 6B f). This indicated that in the hydrous membrane there existed no CH and SA-poor SL phase but there was the SA phase in the left side of this region (probably the left of SL:SA=6:4), in addition to the CH-rich SL and the SA-rich SL phase. It was not really clear whether the latter two would form different phases or one phase rich in both CH and SA. However, if addition of CH to the 5:0:5 (42) mixture, which should not have any CH and SA-poor SL phase, induced formation of the CH-rich SL phase, the proportion of the SA phase would be increased due to extraction of SL from the SA-rich SL phase by CH. When mixtures of SL–CH–SA containing 42% PVP along the line from 5:0:5 (42) to CH(c) in the phase diagram (Fig. 5) were studied on DSC (Fig. 7D), however, the peak assigned to the SA phase was remarkably reduced in height by the addition of CH. This meant that the CH-rich SL phase would not be formed. In addition, it would not be reasonable to consider that the CH-rich SL and the SA-rich SL phases would form different phases in this region where there would not be any CH and SA-poor SL phase, because an SL phase incorporating both CH and SA could exist in the CH(c)-D-E region adjacent to this region as discussed later. The SL phase will be denoted as the CH and SA-rich SL phase (low-CH) in the following: "low-CH" means low CH content. The burst of release and the spouting of droplets observed at 5:0:5 (42) and 2:1:2 (42) (Fig. 5) showed that the SA-rich SL and the CH and SA-rich SL (low-CH) phase could not contribute to prolongation of CCSS release.

CH(c)-A-D Region SL existed here as SL(LCP) saturated with CH, dissolving all the added SA, and excess CH was separated as CH(c) from SL(LCP) in anhydrous membrane mixtures (Fig. 5). The compositions of their membranes in the microcapsules at $Z=0$ to 1 (Figs. 1C, 2C and 4C) were in the CH(c)-A-D region. Their dissolution and swelling behaviors in the area close to the SL–CH(c) line were essentially similar to those in the SL-A-D-B and SA(c)-B-D-E regions. However, the properties in the CH(c)-A-D region were very sensitive to the SA content. Even by addition of such a small amount of SA as $Z=0.25$ (5:5:0.25 (42)), a significant change was found (Figs. 1C and 2C). Addition of SA suppressed the CCSS release and the spouting of the droplets and made microcapsules very swollen especially at the early stage. There was possibly a difference from the role of CH in the SA(c)-B-D-E region as discussed above. However, it should be noted that these effects of SA occurred only when SL(LCP) was saturated with CH in anhydrous state.

When the DSC study was carried out with SL and CH mixtures containing 42% PVP in hydrous state (Fig. 6A), an endothermic peak appeared at 78 °C with the mixture of SL:CH=0:10 (Fig. 6A g). There was a report that CH monohydrate lost its water of hydration at 86 °C, which would be temperature taken at the top of an endothermic peak, consequently forming a high temperature polymorph of anhydrous CH in a closed system of CH monohydrate and water on DSC.[13] Then, the peak at 86 °C was no longer observed on the second run on DSC, but a small endotherm appeared at 36.4 ± 0.5 °C. In our case, the peak at 78 °C appearing on the first run was not observed on the second run, but a small endotherm at 36 °C was detected at SL:CH=0:10 (data not shown). Therefore, the peak at 78 °C would come from CH monohydrate in hydrous state, though CH(c) in anhydrous state was anhydrate.[7] At SL:CH=1:2 and 5:5, the peak was observed at 79 °C with a little increase in temperature, indicating the separation of CH monohydrate in the hydrous membrane (Fig. 6A f and e). Such an increase in CH peak temperature from 76—78 °C of pure CH to 81—82 °C on the first run was also observed in the DSC study using hydrogenated egg lecithin–CH mixtures.[9e] At SL:CH=6:4 and 5:2, however, the peak at 78—79 °C was no longer detected (Fig. 6A d and c), although CH(c) was detected in anhydrous membrane with SL:CH=4:1 or more CH on DSC. Bourges *et al.* reported that the amount of CH which could be incorporated into lecithin was increased to 27% in excess water from 18% in the dry lecithin–CH system.[9d] This indicated that in hydrous state the saturation point moved to higher CH content (Fig. 5).

DSC thermograms are shown in Fig. 7C when mixtures of 5:5:Z (42) in hydrous state were studied on DSC. At $Z=0$ and 0.25 (5:5:0 (42) and 5:5:0.25 (42)), small endothermic peaks were observed at 79 °C (Fig. 7C a and b). Behavior of the thermograms at $Z=0$ and 0.25 were the same as that at SL:CH=0:10 both on the first (Fig. 6A g) and the second run (data not shown), although there was a little increase in temperature on the former and a

little decrease on the latter. Therefore, the peak at 79 °C would come from CH monohydrate separated from SL in hydrous state. According to Bourges *et al.*,[9d] the lamella phase composed of lecithin and CH should coexist with CH crystals: the former corresponded to the CH-rich SL phase and the latter to CH monohydrate in this study. The burst of CCSS release (Fig. 1C) and the spouting of droplets at $Z=0$ showed that the CH-rich SL phase containing no SA could not contribute to prolongation of CCSS release. Disappearance of the peak at 79 °C at $Z=0.5$ (5:5:0.5 (42)) would not be due to decrease in proportion of CH monohydrate in the mixtures with increase in SA, because only a small amount of SA was added at $Z=0.5$ (Fig. 7C c). This suggested the dissolution of CH monohydrate in SL together with SA, its formation of non-crystalline mixture with SA, or its transformation to the anhydrate. However, the peak around 36 °C attributable to polymorphic crystalline transition of the CH anhydrate was detected neither in Fig. 7C c nor on the second run (data not shown). Further, it was found that CH containing SA could not become completely non-crystalline, when CH–SA mixtures containing 42% PVP were studied on DSC (Fig. 6C). Considering that no CH-poor SL existed at $Z=0$ but did in the CH-rich SL phase and the CH monohydrate, there was only one possibility that the crystalline CH phase disappeared by forming a CH and SA-rich SL phase by hydration at $Z=0.5$. In addition, the fact that the separated CH-rich SL and SA-rich SL phases could not contribute to suppression of the release and the spouting, as seen at 5:5:0 (42) (Figs. 1C and 4C) and 5:0:5 (42) (data not shown but mentioned in the SA(c)-B-D-E region), supported the formation of this mixed phase. Then, since SA content in the CH and SA-rich SL phase was still low, no peak on DSC appeared. When SA increased to $Z=1$ (5:5:1 (42)), a very broad and small peak centered at 48 °C was observed (Fig. 7C e). As discussed in the SL–SA–PVP system (Fig. 6B), this indicated the SL–SA complex formation (SA-rich SL phase). This phase, the CH and SA-rich SL phase containing a small amount of SA, will be denoted below as the CH and SA-rich SL (low-SA) phase.

A large number of small, colorless droplets also remained surrounding microcapsules after spouting of yellow droplets with microcapsules at 6.3:3:0.7 (42), but only a few with those at 5.6:3:1.4 (42) in this region (data not shown but plotted in Fig. 5), similar to those at $Y=0$, 1 and 2 (Fig. 3 e and f). The small, colorless droplets appeared around 20 min after immersion with the former and around 45 min with the latter. In these cases, SL content in their membranes was high, about 55—70%. These seemed to suggest that the microcapsules with 55—70% SL were eroded with the release of their membrane materials as the small, colorless droplets in the solution. This would account for the phenomenon that in the area close to the boundary of A-D, the CH and SA-poor SL, the CH-rich SL and the SA-rich SL phases would exist as in the SL-A-D-B region.

CH(c)-D-E Region In the CH(c)-D-E region the microcapsule membranes at $Y=2$ to 16 (Figs. 1B, 2B, 3e, 3f and 4B) and $Z=2$ to 5 (Figs. 1C, 2C, 3c, 3d and 4C) were included. All microcapsules, except for those at $Y=2$ (5:2:2 (42)), showed significantly prolonged release of CCSS with a lag time (Figs. 1B, 1C, 2B and 2C) and were remarkably swollen (Figs. 4B and 4C) with no spouting of yellow droplets at the early stage of immersion in the solution (Fig. 3c and 3d).

In this region SL existed as SL(LCP) saturated with both CH and SA, and CH(c) and SA(c′) were separated from SL(LCP) in anhydrous membrane mixtures (Fig. 5). Therefore, the prolonged-release characteristics in this region would relate to saturation of SL(LCP) with both of them.

In the hydrous membrane mixtures changed at 5:5:Z (42), a broad peak centered at 59 °C was found at $Z=2$ on the DSC thermogram (Fig. 7C f). With increase in SA, the peak was shifted to a higher temperature (Fig. 7C g and h). It appeared at 55 °C and was likely to be composed of two peaks at $Z=4$ and 5 (Fig. 7C h and i) as seen in Fig. 6B e—h. As discussed in the CH(c)-A-D region, it would be inferred that the peak observed as a slowly declining edge or a shoulder at the lower temperature side of the peak of separated SA phase was attributed to the SA-rich SL phase formed in the solution. Existence of two peaks was more clearly established on a thermogram with the mixture of 1:3:1 (42) in this region (Fig. 7D d). At $Z=2$ to 5, the peak at 78—79 °C, which was attributable to separated CH monohydrate in the hydrous membrane, was not observed on the thermograms (Fig. 7C f—i), similar to $Z=0.5$ to 1 (Fig. 7C c—e). It was also suggested that CH would be dissolved to form the CH and SA-rich SL phase by addition of SA and hydration. Separation of CH monohydrate was observed in the hydrous membrane mixtures only at such a high CH content as $Y=16$ (Fig. 7B g), 0.5:9:0.5 (42) and 1:8:1 (42) (Fig. 7D b and c) in this region. On the other hand, while separation of SA was detected at $Z=2$ or more in anhydrous state,[7] it was not clearly observed even at $Z=3$ in hydrous state (Fig. 7C g). These results suggested that the capacity of SL to incorporate SA might be increased by hydration and, consequently, that the boundary CH(c)-B showing the appearance of SA phase might move to the left side of the diagram, passing between $Z=3$ and $Z=4$ and terminating around SL:SA=6:4 on the boundary SL–SA(c) in hydrous state (Figs. 7C g and h and 6B f).

When CH and SA mixtures containing 42% PVP hydrated in a 0.9% saline solution were studied on DSC, the endothermic peak appeared at 67 °C at CH:SA=0:10 (Fig. 6C g), which was the same as that with SA alone in anhydrous state.[7] At CH:SA=9:1, three endothermic peaks at 57 °C, 67 °C and 82 °C were observed (Fig. 6C b). The peaks at 67 °C and 82 °C would come from separated SA and CH monohydrate, respectively, (Fig. 6C g and a). At CH:SA=3:1 and 5:5, the peak at 82 °C disappeared and only two peaks at 57 °C and 67 °C were detected without changes in the transition temperatures (Fig. 6C c and d); these two peaks increased in peak area with SA content. Then, the area of the peak at 57 °C was reduced with increase in the SA fraction beyond CH:SA=5:5 (Fig. 6C e and f), while that at 67 °C was increased. The peak at 57 °C suggested some interaction between CH and SA or formation of the CH–SA mixture by hydration, since such a change on the thermogram was

not observed in anhydrous state.[7] Further, when the mixture of $X:5:5$ (42) in hydrous state were studied on DSC, the peak at 57 °C was shifted to a lower temperature by addition of even a small amount of SL such as $X=1$ (Fig. 7A b). At $X=2$, the peak was reduced to a broad shoulder on the peak at 67 °C (Fig. 7A c). The area of this shoulder was increased until $X=12.5$ with decrease in the area of the peak at 67 °C (Fig. 7A f). These results suggested that the CH and SA-rich SL phase was increased in proportion with increase in SL content up to $X=12.5$, accompanying the decrease in the SA phase. Figure 7A g and h also showed that the SA-rich SL phase coexisted with the CH and SA-poor SL phase above $X=12.5$, since the peak shifted to lower temperature.

In this region, there would be potential for formation of the CH and SA-rich SL and the SA phases in a hydrated microcapsule membrane. The remarkable swelling of microcapsules observed in this region would be attributable to the CH and SA-rich SL phase reconstructed from SL saturated with CH and SA in anhydrous state. The suppression of spouting of the yellow droplets immediately after immersion would result from absence of the CH and SA-poor SL, the CH-rich SL, the SA-rich SL and the CH and SA-rich SL (low-CH or SA) phases. In the part close to the boundary CH(c)–D, there would exist the same phases as those in CH(c)-A-D region: the CH and SA-rich SL (low-SA) phase. SA content in the CH and SA-rich SL (low-SA) phase would not be high enough to completely suppress the delayed spouting of droplets. The CH crystalline phase existed only in the area close to the CH(c) apex.

The microcapsules at $Y=2$ (Fig. 1B, 3e, 3f and 4B) and 2:1:2 (42) (data not shown, but plotted in Fig. 5) showed rapid release, a slight expansion and spouting of yellow droplets immediately after immersion, although compositions of their membranes were in the CH(c)-D-E region. As discussed in the CH(c)-A-D region, it would be suggested that in the area of CH(c)-D-E close to the boundary A-C on the phase diagram (Fig. 5), there would exist the CH and SA-poor SL, the CH-rich SL and the SA-rich SL phases on the right side and the CH and SA-rich SL (low-CH) and the SA phases on the left; there would be a small amount of the CH and SA-poor SL at $Y=2$. This could be one reason that the microcapsules at $Y=2$ and 2:1:2 (42) showed dissolution properties similar to those in the SA(c)-B-D-E region. At $Y=2$ the small, colorless droplets remained surrounding microcapsules after spouting of the yellow droplets, as seen at $Y=0$ and 1, but not for 2:1:2 (42). This would be due to a difference in SL content: it was 55% at $Y=2$ and 40% at 2:1:2 (42).

Yellow droplets were not observed at the early stage, but almost colorless ones were seen at a little later stage at $Y=3$, 5 and 7, and at $Z=2$ and 3, possibly leading to erosion of the microcapsules and faster decrease in SR after reaching MSR in swelling studies (Figs. 4B and 4C). It was not clear whether the droplets contained CCSS or not. In these microcapsules, membranes were composed of SL(LCP) which was saturated with both CH and SA and separated crystals of CH and SA in anhydrous state. When they were immersed in the solution, the CH and SA crystals disappeared (Figs. 7B d, e and f and 7C f and g), and subsequently the CH and SA-rich SL (low-SA) phase would be formed and spouted with a lag time.

No spouting of the droplets was observed at $Y=16$, in contrast to the microcapsules at $Y=3$, 5 and 7 and $Z=2$ and 3. The DSC thermogram exhibited two peaks, possibly assigned to the CH and SA-rich SL phase and CH monohydrate (Fig. 7B g). This should relate to the prolonged swelling as seen in Fig. 4B. The prolonged swelling (Fig. 4B) and release (Fig. 1B) would be attributable to reduced water-permeability of the membrane caused by the separated CH monohydrate, a high content of CH in the CH and SA-rich SL phase and a low SL content (22%).

CH(c)-C-E Region In the CH(c)-C-E region, CH and SA were separated in anhydrous membrane mixtures as in the CH(c)-D-E region; two different SA crystalline phases, SA(c) and SA(c′), existed (Fig. 5). Existence of SL(LCP), however, could not be confirmed by DSC, XRD or microscopy.[7]

Microcapsules were prepared at $X=0$ to 2 (Figs. 1A, 2A and 4A) and $Z=15$ to 18.5 (Figs. 1C, 2C and 4C). When the microcapsule membrane had the composition close to the boundary CH(c)–SA(c) on the phase diagram (Fig. 5), such as $X=0$ and 1 (0:5:5 (42) and 1:5:5 (42)), the microcapsules were bursting devices in spite of being non-swelling and non-spouting (Figs. 1A, 3a, 3b and 4A). A low proportion of the SL phase would account for these behaviors. As the content of SL in the membrane increased to about 20% ($X=2$ and $Z=15$, 2:5:5 (42) and 5:5:15 (42), respectively), microcapsules became long-term prolonged-releasing and largely, slowly swelling devices (Figs. 1A, 1C, 4A and 4C). The microcapsules at $Z=18.5$ (5:5:18.5 (42)) were on the border between the CH(c)-C-E and SA(c)-C-E regions.

When microcapsule membranes were hydrated, the CH and SA-rich SL and the SA phases would be formed in this region. Figure 7A a and b strongly support the existence of these phases. CH crystalline phase existed only in the upper part of this region (Fig. 6C b). The prolonged and large swelling of the microcapsules at $X=2$ and $Z=15$ probably related to slow hydration of the CH and SA-rich SL phase caused by loading a large amount of CH and SA, and it would be responsible for the delayed and slow release of CCSS. These behaviors were similar to microcapsules at 1:3:1 (42) in the CH(c)-D-E region, about 20% of whose membrane was SL. Therefore, it was also suggested that microcapsules would be swollen slowly to the largest size when the SL content in membranes was about 20% and the CH and SA-rich SL phase was formed.

SA(c)-C-E Region Anhydrous membrane mixtures in the SA(c)-C-E region had the crystalline phases: SA(c) and SA(c′) (Fig. 5). SL(LCP) was not confirmed by DSC, XRD or microscopy.[7] Microcapsules were prepared at $Z=25$ and 40 (5:5:25 (42) and 5:5:40 (42), Figs. 1C, 2C, 3k, 3l and 4C). When microcapsules with the membrane in this region contacted water, the CH and SA-rich SL and the SA phases would be formed in the membrane (Fig. 7C). The rapid CCSS release and slight swelling of the microcapsules indicated that the former phase would be the CH and SA-rich SL (low-CH) phase.

Effect of PVP In the previous study,[7] there was little

meaningful effect of PVP on the phase separation in anhydrous membrane mixtures at 5:5:2 (P). However, the present study showed that PVP contributed strongly to release suppression (Fig. 1D) and swelling (Fig. 4D). The solubility study showed most PVP to be separated from the other components in anhydrous membrane. At $P=10$, 20, 30, 42, 50 and 60, PVP accounted for 9.1, 16.7, 23.1, 29.6, 33.3 and 37.5% of membrane volume, respectively, assuming an equal density of all components. According to the percolation theory, the particulate system of randomly-packed two-components of the same size has a three-dimensional lower percolation threshold at 20—43% (v/v) or 10—39% (v/v) in site or bond percolation, respectively, depending on the lattice type.[8] Figure 2D seemed to suggest the percolation threshold existed around $P=40$. At low content such as $P=10$ or 20, the PVP phase would be isolated; therefore, the coexisting CH and SA-rich SL phase could swell quickly, leading to the fast swelling of microcapsules (Fig. 4D) and the frequent spouting of droplets, even if SL : CH : SA = 5 : 5 : 2. While the PVP phase would become more interconnective with increase in PVP, the SL phase would became more isolated and more finely dispersed in the membrane, but still open to the outside of the membrane, leading to easier spouting of droplets; consequently, the spouting became most frequent at $P=30$. The spanning-clusters of PVP phases growing above $P=30$ would, in contrast, delay the swelling and prolong the CCSS release, perhaps because the developed spanning-clusters of PVP phases would prevent the SL phase from extruding out of the membrane.

Possible Major Phases in Hydrous SL–CH–SA System Incorporating 42% PVP The major phases possibly formed in the SL–CH–SA system incorporating 42% PVP by hydration were summarized in a phase diagram (Fig. 8). Existence of the CH and the SA phases was confirmed by the endothermic peaks which were attributable to CH monohydrate and SA crystal, respectively, in DSC study. Formation of the following SL phases was suggested by the DSC study and several reports:[9a-c,10-12] the CH and SA-poor SL; the CH-rich SL; and the SA-rich SL. Furthermore, formation of the CH and SA-rich SL phase was estimated from the DSC study and the release and swelling properties of microcapsules.

Relation of SL Content with T_{lag} and MSR T_{lag} is plotted against SL content in Fig. 9A. Open symbols show the microcapsules which have membranes containing only the CH and SA-rich SL as SL phase dissolving a large amount of CH and SA and, therefore, from which the spouting of the droplets was not observed at the early stage. T_{lag} was large at an SL content of 20 to 45% (II): the largest T_{lag} was 75 min with microcapsules of 1 : 3 : 1 (42) containing 20% SL. T_{lag} was rapidly reduced as SL content decreased below 20% (I) or increased above 45% (III). However, small T_{lag} was observed even with the microcapsules containing 20—45% SL when the mem-

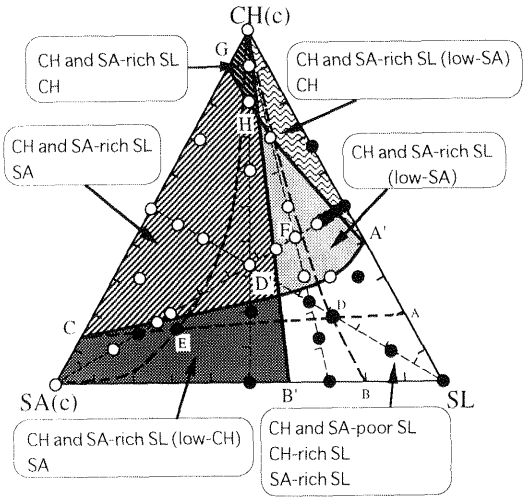

Fig. 8. Estimated Major Phases in Hydrous SL–CH–SA System Incorporating 42% PVP

The closed and open symbols are the same as those in Fig. 5. The major phases possibly existing in each region are shown: zone SL-A'-D'-B', CH and SA-poor SL, CH-rich SL and SA-rich SL; zone SA(c)-B'-D'-C, CH and SA-rich SL (low-CH) and SA; zone A'-D'-H, CH and SA-rich SL (low-SA); zone CH(c)-A'-H, CH and SA-rich SL (low-SA) and CH; zone C-D'-H-G, CH and SA-rich SL and SA; zone CH(c)-G-H, CH and SA-rich SL and CH. It was not clear in zone SL-A'-D'-B' whether the CH-rich SL and the SA-rich SL phases were separated or formed one SL phase, the CH and SA-rich SL (low-CH and SA) phase.

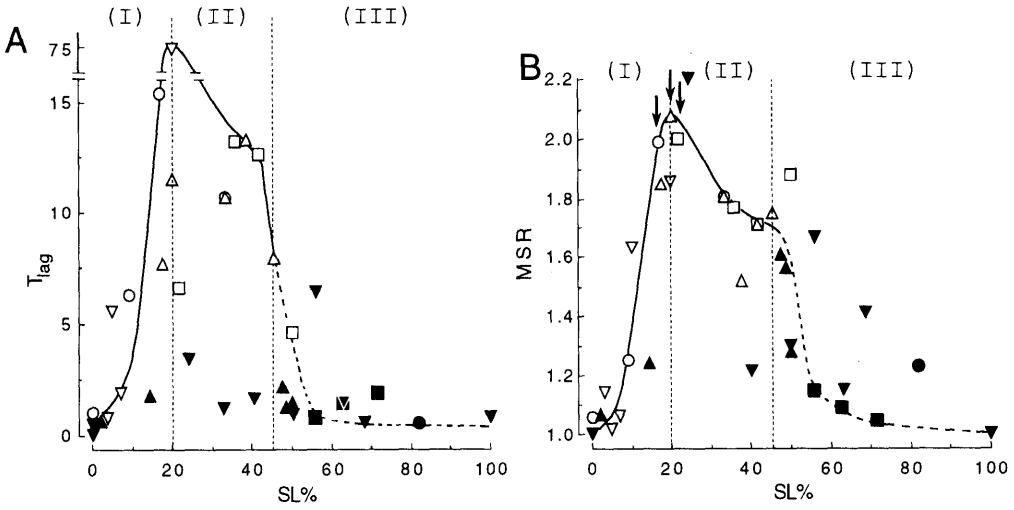

Fig. 9. Relation of SL Content in a Membrane with T_{lag} (A) or MSR (B)

Composition of a membrane was changed: ●, ○, X:5:5 (42); ■, □, 5:Y:2 (42); ▲, △, 5:5:Z (42); ▼, ▽, others. Open symbols, microcapsules with only CH and SA-rich SL dissolving a great amount of CH and SA as SL phase; closed, others. Arrowed symbols in (B) show the microcapsules whose SR was still increasing at the end of the observation period.

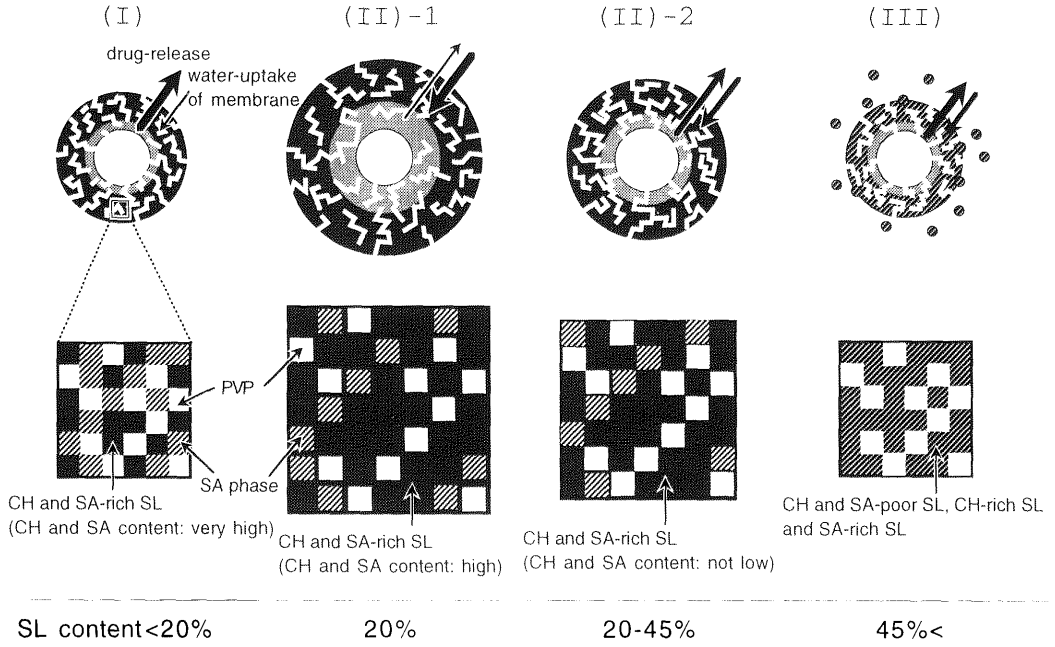

Fig. 10. Schematic Diagram of Estimated Release Mechanisms of Microcapsules Depending on SL Content When the Composition Changed at X: 5 : 5 (42)

brane contained the CH and SA-poor SL, the CH-rich SL and/or the SA-rich SL phases (closed symbols in Fig. 9). The relation of MSR to SL content is shown in Fig. 9B, indicating that MSR was more strongly correlated to the SL content. This relation was similar in profile to that between T_{lag} and SL content. When SL content was 20—45% (II), microcapsules were also extremely swollen: the largest swelling was observed around 20% SL content. MSR was sensitive to SL content rather than to what kind of SL phase existed.

Estimated Release Mechanisms A schematic diagram of estimated release mechanisms is shown in Fig. 10, typically when the membrane composition changed at X: 5 : 5 (42). Membranes were mainly occupied by PVP and the separated CH and SA, and the SL phase existed in only a small amount in anhydrous state when SL content was less than 20% (Fig. 10 (I)). When the membrane was hydrated, the separated CH disappeared, which would be incorporated in SL together with some amount of SA. Consequently, the CH and SA-rich SL phase whose CH and SA content was very high would be formed, but it could not lead to any overall swelling of membrane and could not act as a diffusion barrier due to its low SL-content (Fig. 9B (I)). In this case, CCSS was rapidly released through the spaces possibly resulting from PVP release or the hydrated PVP phase and the gaps between each phase. When SL content reached 20%, the separated CH in the anhydrous membrane would also be incorporated in the SL phase by hydration as in case (I). Then, the CH and SA-rich SL phase whose CH and SA content was high would also be formed by hydration (Fig. 10 (II)-1), but its CH content would be lower than in case (I). During large and slow swelling of the CH and SA-rich SL phase (Fig. 9B (II)), the CCSS release from microcapsules were suppressed (Fig. 9A (II)). Consequently, the swollen membrane would act as a strong diffusion-barrier. This would account for the most prolonged release with a large T_{lag} at 20% of SL content. With increase in SL content (Fig. 10 (II)-2), the content of CH incorporated in the CH and SA-rich SL phase in the hydrous membrane would be lowered. The faster swelling (Fig. 9B (II)), that is, faster water-uptake of the CH and SA-rich SL phase whose CH and SA content was lowered would result in the faster release of CCSS and less swelling as seen with more than 20% SL (Fig. 9A (II)). The difference in the swelling rate and degree between (II)-1 and (II)-2 would be caused by reduction of the CH and SA contents incorporated in the CH and SA-rich SL phase. As SL content increased to more than 45% (Fig. 10 (III)), the CH and SA-poor SL, the CH-rich SL and the SA-rich SL phases would be separated, leading to spontaneous spouting of droplets, and the release rate of CCSS was greatly increased (Fig. 9A (III)). Small MSR as seen in Fig. 9B (III) would be attributable to the spouting of the SL phase as droplets at the early stage.

Conclusion

Microcapsules whose membranes consisted of SL, CH, SA and PVP were prepared with broadly varying compositions. Dissolution and swelling behaviors of the microcapsules in a 0.9% saline solution were related with the phase diagram which were estimated using anhydrous membrane mixtures studied previously.[7] Possible structural and physico-chemical features of the hydrated microcapsule membrane were also estimated. When microcapsules had membranes composed of SL(LCP) unsaturated with both CH and SA, or saturated with only one of them in anhydrous state, they showed a rapid release of CCSS, a minimal swelling, and spouting of droplets in the solution. These behaviors were observed in SL-A-D-B, SA(c)-B-D-E, CH(c)-A-D and SA(c)-C-E regions on the phase diagram. The CH and SA-poor SL, the CH-rich SL, the SA-rich SL and the CH and SA-rich SL (low-CH or SA) phases formed in these regions by

hydration were estimated to contribute to the rapid release and spouting of droplets. A significantly delayed release and a large swelling of microcapsules without spouting of the droplets containing CCSS at the early stage were observed in the CH(c)-D-E and CH(c)-C-E regions, where the microcapsule membranes were composed of SL(LCP) saturated with both CH and SA in anhydrous state, except for the area close to the borders, CH(c)–SA(c), CH(c)-B and C-A; the latter two seemed to be shifted by hydration. In these regions, the CH and SA-rich SL phase was estimated to be formed by hydration, leading to the significantly delayed release and the great swelling. The degree of release suppression and MSR depended on the SL content. With SL content of 20—45%, the CH and SA-rich SL phase was extremely swollen and would act as a strong diffusion-barrier. It was further suggested that PVP would be contributable to the prolonged release and the great swelling, when its content was above the lower percolation threshold.

By varying the composition of the membranes, it was possible to regulate dissolution, swelling and erosion behaviors of the microcapsules flexibly and easily. The microcapsules will be useful as a dosage form, for instance, for chemoembolization therapy of cancer, where individualized alteration of a dissolution profile and degradation behavior of the dosage form is required depending on the disease state of a patient.

Acknowledgments This work was supported in part by a Grant-in-Aid for Cancer Research (6—15) from The Japanese Ministry of Health and Welfare, Grants-in-Aid for Scientific Research (05671798), (B) (08457598) and (C) (09672204) from The Japanese Ministry of Education, Science, Sports and Culture, a Grant-in-Aid from the Hosokawa Powder Technology Foundation and a Grant-in-Aid for Health Science from Kobe Gakuin University.

References

1) Washington C., *Advan. Drug Delivery Rev.*, **20**, 131—145 (1996).
2) Lasic D. D. (ed), "Liposome: from Physics to Applications," Elsevier, Netherlands, 1993.
3) *a*) Fujii M., Terai H., Mori T., Sawada Y., Matsumoto M., *Chem. Pharm. Bull.*, **36**, 2186—2192 (1988); *b*) Fujii M., Harada K., Yamanobe K., Matsumoto M., *ibid.*, **36**, 4908—4913 (1988); *c*) Fujii M., Harada K., Matsumoto M., *ibid.*, **38**, 2237—2241 (1990); *d*) Fujii M., Harada K., Kakinuma K., Matsumoto M., *ibid.*, **39**, 1886—1888 (1991); *e*) Fujii M., Hasegawa J., Kitajima H., Matsumoto M., *ibid.*, **39**, 3013—3017 (1991); *f*) Fujii M., Hioki M., Nishi M., Henmi T., Nakao M., Shiozawa K., Matsumoto M., *ibid.*, **41**, 1275—1278 (1993).
4) *a*) Nishihata T., Wada H., Kamada A., *Int. J. Pharm.*, **27**, 245—253 (1985); *b*) Nishihata T., Sudho M., Kamada A., Keigami M., Fujimoto T., Kamide S., Tastumi N., *ibid.*, **33**, 181—186 (1986); *c*) Nishihata T., Keigami M., Kamada A., Fujimoto T., Kamide S., Tatsumi N., *ibid.*, **42**, 251—256 (1988).
5) Fukumori Y., Ichikawa H., Jono K., Tokumitsu H., Shimizu T., Kanamori R., Tsutsumi Y., Nakamura K., Murata K., Morimoto A., Tsubakimoto M., Nakatsuka H., Minakuchi K., Onoyama Y., *Chem. Pharm. Bull.*, **42**, 2604—2611 (1994).
6) *a*) Fukumori Y., Fukuda T., Hanyu Y., Takeuchi Y., Osako Y., *Chem. Pharm. Bull.*, **35**, 2949—2957 (1987); *b*) Fukumori Y., Yamaoka Y., Ichikawa H., Fukuda T., Takeuchi Y., Osako Y., *ibid.*, **36**, 1491—1501 (1988); *c*) Fukumori Y., Yamaoka Y., Ichikawa H., Takeuchi Y., Fukuda T., Osako Y., *ibid.*, **36**, 3070—3078 (1988); *d*) *Idem.*, *ibid.*, **36**, 4927—4932 (1988); *e*) Fukumori Y., Ichikawa H., Yamaoka Y., Akaho E., Takeuchi Y., Fukuda T., Kanamori R., Osako Y., *ibid.*, **39**, 164—169 (1991); *f*) *Idem.*, *ibid.*, **39**, 1806—1812 (1991); *g*) Fukumori Y., Ichikawa H., Jono K., Takeuchi Y., Fukuda T., *ibid.*, **40**, 2159—2163 (1992); *h*) Fukumori Y., Ichikawa H., Jono K., Fukuda T., Osako Y., *ibid.*, **41**, 725—730 (1993); *i*) Ichikawa H., Jono K., Tokumitsu H., Fukuda T., Fukumori Y., *ibid.*, **41**, 1132—1136 (1993); *j*) Fukumori Y., Ichikawa H., Tokumitsu H., Miyamoto M., Jono K., Kanamori R., Akine Y., Tokita N., *ibid.*, **41**, 1144—1148 (1993); *k*) Ichikawa H., Tokumitsu H., Jono K., Fukuda T., Osako Y., Fukumori Y., *ibid.*, **42**, 1308—1314 (1994).
7) Jono K., Ichikawa H., Fukumori Y., Kanamori R., Tsutsumi Y., Murata K., Morimoto A., Nakamura K., *Chem. Pharm. Bull.*, **44**, 392—398 (1996).
8) *a*) Stauffer D., Aharony A., "Introduction to Percolation Theory," 2nd ed, Taylor & Francis, London and Washington D.C., 1991; *b*) Leuenberger H., Rohera B. D., Haas Ch., *Int. J. Pharm.*, **38**, 109—115 (1987); *c*) Caraballo I., Holgado M. A., Fernández-Arévalo M., Millán M., Rabasco A. M., *Drug Develop. Ind. Pharm.*, **23**, 1—8 (1997).
9) *a*) Mabrey S., Mateo P. L., Sturtevant J. M., *Biochemistry*, **17**, 2464—2468 (1978); *b*) McMullen T. P. W., McElhaney R. N., *Biochim. Biophys. Acta*, **1234**, 90—98 (1995); *c*) Phillips M. C., Finer E. G., *ibid.*, **356**, 199—206 (1974); *d*) Bourgés M., Small D. M., Dervichian D. G., *ibid.*, **137**, 157—167 (1967); *e*) Khan M. Z. I., Tucker I. G., *Chem. Pharm. Bull.*, **40**, 3056—3061 (1992); *f*) Freeman R., Finean J. B., *Chem. Phys. Lipids*, **14**, 313—320 (1975).
10) Schullery S. E., Seder T. A., Weinstein D. A., Bryant D. A., *Biochemistry*, **20**, 6818—6824 (1981).
11) Mabrey S., Sturtevant J. M., *Biochim. Biophys. Acta*, **486**, 444—450 (1977).
12) Zuidam N. J., Crommelin D. J. A., *Int. J. Pharm.*, **126**, 209—217 (1995).
13) Loomis C. R., Shipley G. G., Small D. M., *J. Lipid Res.*, **20**, 525—535 (1979).